Implications of Input Neurons' Spike Timing Synchrony for Neural Coding

Ruixin Zhang, Stephen Lisberger

INTRODUCTION

Purkinje cells reside in the cerebellar cortex. They release inhibitory signals in the form of neurotransmitter GABA (gamma-aminobutyric acid) to their target neurons in the cerebellar nuclei [1]. During smooth pursuit eye movements, there is a reciprocal relationship between the activity of Purkinje cells and their downstream neurons, called floccular target neurons [2]. When a moving object is detected in the visual field, Purkinje cells inhibit floccular neurons. This inhibition decreases the excitatory drive to downstream motor neurons that control eye movements, slowing the eyes down and allowing them to track the moving object. Together, these 2 types of neurons modulate the precision and accuracy of smooth pursuit eye movements, playing a crucial role in the fine-tuning of eye movements.

Purkinje cells encode information using both rate codes and temporal codes [3]. The firing rate of Purkinje cells, or rate codes, can be modulated by the amplitude of eye movements during smooth pursuit. The timing of the firing of Purkinje cells, or temporal codes, can represent information about precisely timed sensory or motor events. Person and Raman's paper in 2011 demonstrates that the synchrony of spike timing of Purkinje cells could be an important part of the neural code for the output from the cerebellar cortex [4]. My goal is to test Person's theory by asking how synchrony affects the resting discharge properties of target neurons of Purkinje cells.

My strategy is to create a simple Python model that can simulate a real neuron and then to control the synchrony of inhibitory inputs in the model and ask how it affects the resting discharge properties of a target neuron. I create an artificial neural network with a large number of inhibitory and excitatory neurons that feed into a single target neuron [5]. I then tune the values of neuronal properties, like synapse conductances, number of neurons, and length of afterhyperpolarization periods, to make my model match up with a real target neuron recording in a behaving animal, in vivo. I successfully simulate the resting discharge properties of this real target neuron without involving synchrony in my model.

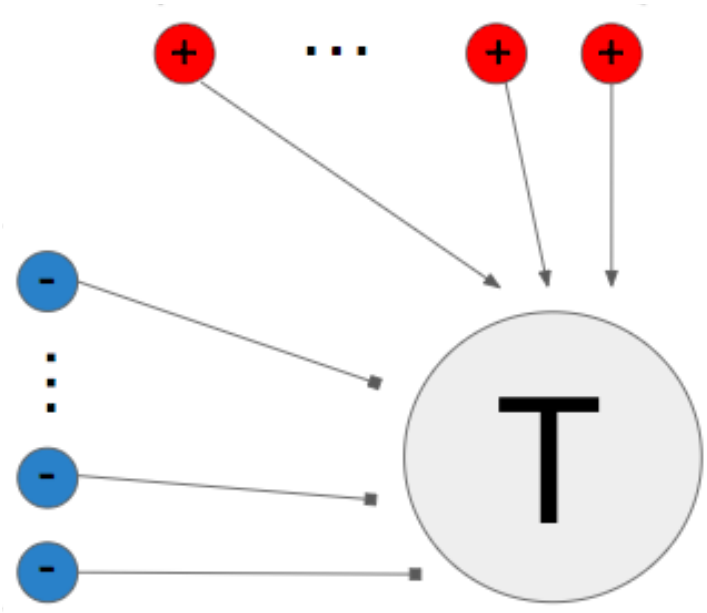

Figure 1: The Model. "T" designates a target neuron that receives inputs from a large number of excitatory neurons (red) and inhibitory neurons (blue).

My results indicate that adding synchrony of inhibitory inputs (simulating synchronized Purkinje cells' firing rates), makes the resting discharge of the model target neuron become more different from the neuron recording. Little or no inhibitory input synchrony is required to match the resting firing statistics of the model neuron to those of the real neurons. Therefore, I conclude that the synchrony of inhibitory inputs may not be a major component of the neural code for the output from the cerebellum.

METHODOLOGY

We simulate a model consisting of excitatory and inhibitory inputs to a single target neuron. Our goal is to understand how the spiking patterns of the input neurons could work together to generate spiking patterns in the target neuron that reproduce recordings made from behaving animals, in vivo.

The spike patterns of excitatory and inhibitory input neurons are randomized and generated at runtime according to the following equations:

$$n_E = 45, \; n_I = 40 \quad (1)$$
$$t_{Ei} = 0.03 + 0.045/n_E * i \quad (2)$$
$$S_{Eij} = t_{Ei} * j + randint(100, 400)/1000 \quad (3)$$
$$t_{Ii} = 0.03 + 0.04/n_I * i \quad (4)$$

$$S_{Iij} = t_{Ii} * j + randint(100, 400)/1000 \quad (5)$$

where n_E is the number of excitatory neurons, n_I is the number of inhibitory neurons. The simulation includes more excitatory neurons than inhibitory neurons to ensure that there's more excitation than inhibition, allowing the target neuron to achieve a spike rate of around 40 spikes per second. t_{Ei} is the interspike time interval for the ith excitatory neuron. This equation is a simple way of ensuring each excitatory neuron has a different mean spike rate, with the maximum spike rate being 1000/30 = 33.3 spikes/second and the minimum spike rate being 1000/75 = 13.3 spikes/second. S_{Eij} is the time point of the jth spike for ith excitatory neuron. As a neuron's interspike interval has slight variations across time, the added random numbers in (3) and (5) simulate this property. The equations for inhibitory neurons follow a similar logic. The coefficients are set empirically, and the units are seconds for (2), (3), (4), (5).

We simulate the target neuron according to the following equations:

$$J_{in}(t) = J_R + J_C + J_{rev} \quad (1)$$
$$J_{in}(t) = [V(t) - V_{rest}]/R + C * [dV(t)/dt] +$$
$$[V(t) - E_{EPSP}] * g_{EPSP} + [V(t) - E_{IPSP}] * g_{IPSP} \quad (2)$$
$$C = \tau/R \quad (3)$$

This set of equations updates the incoming current. $J_{in}(t)$ is total incoming current, which consists of resistor's current J_R, capacitor's current J_C, and reversal potential induced current J_{rev}. A parallel circuit of a resistor and a capacitor is a model for a leaky integrate and fire neuron. $V(t)$ is current membrane voltage, V_{rest} is the resting membrane voltage, R is resistance, C is capacitance, τ is the resistive-capacitive time constant. In addition, I add reversal potential current to encapsulate the property of neurons with a reversed direction of net current flow at such potentials. E_{EPSP} and E_{IPSP} are the excitatory and inhibitory synapse reversal potentials. g_{EPSP} and g_{IPSP} are the excitatory and inhibitory synapse conductance. By convention, V_{rest} is set to -70mV, R is 1Ω, τ is $10 + 20 * rand(0, 1)$ ms, dt is 0.1 ms, E_{EPSP} is 0 mV, E_{IPSP} is -80mV, g_{EPSP} is 10S, and g_{IPSP} is 20S.

Rearranging the set of equations for the target neuron yields a set of equations that update the membrane voltage of the target neuron before hyperpolarization, when ahp_{time}, the time remaining in the afterhyperpolarization period is 0.

$$(ahp_{time} = 0)$$
$$dV(t) = 1/\tau * (J_{in}(t) * R + [V_{rest} - V(t)] + g_{EPSP} * R * [E_{EPSP} - V(t)] +$$
$$g_{IPSP} * R * [E_{IPSP} - V]) * dt \quad (1)$$

$$V(t) = V(t) + dV(t) \quad (2)$$

When the target neuron fires, ahp_{time}, the time remaining in the afterhyperpolarization period is reset to t_{ahp}, the length of the afterhyperpolarization period. (2) and (3) are under the condition that we are still in the afterhyperpolarization period, with $V(t)$ set at resting potential, unaffected by incoming excitatory or inhibitory spikes, and time left in the afterhyperpolarization period keeps decreasing:

$$ahp_{time} = t_{ahp} \quad V(t) > V_{thresh} \quad (1)$$
$$(ahp_{time} > 0)$$
$$V(t) = V_{rest} \quad (2)$$
$$ahp_{time} = ahp_{time} - dt \quad (3)$$

RESULTS

a.

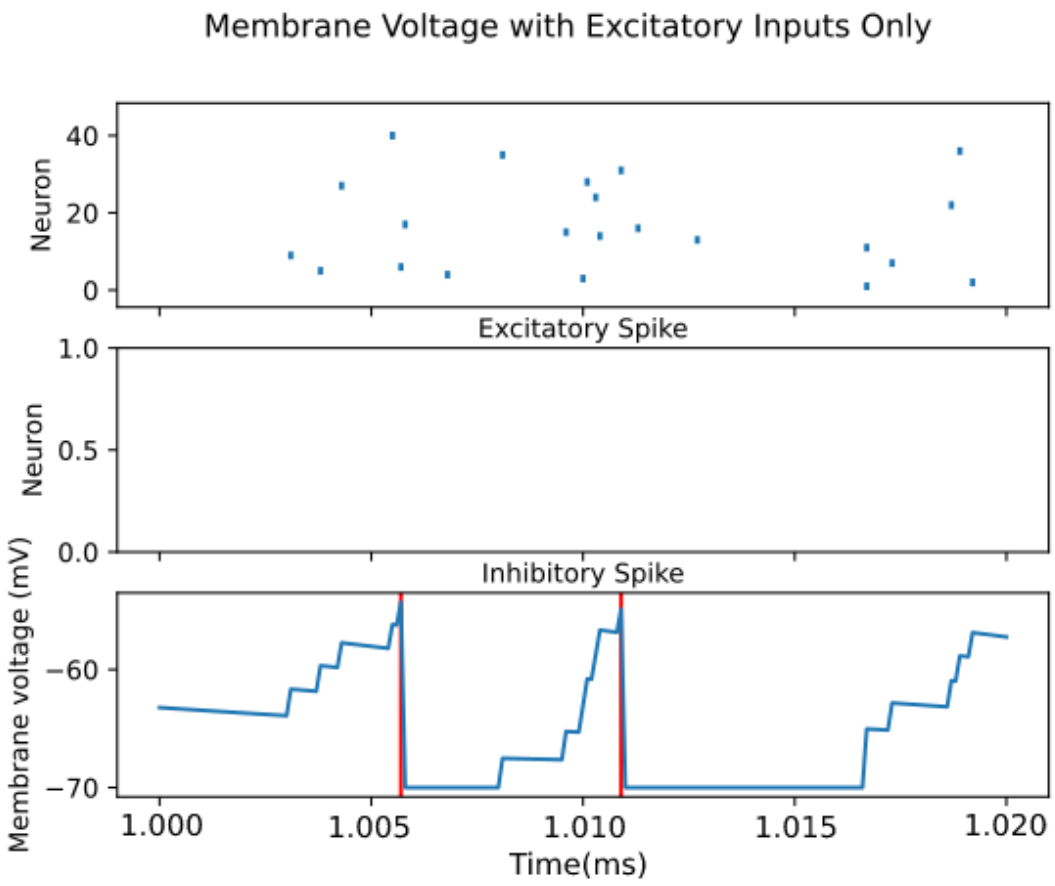

b.

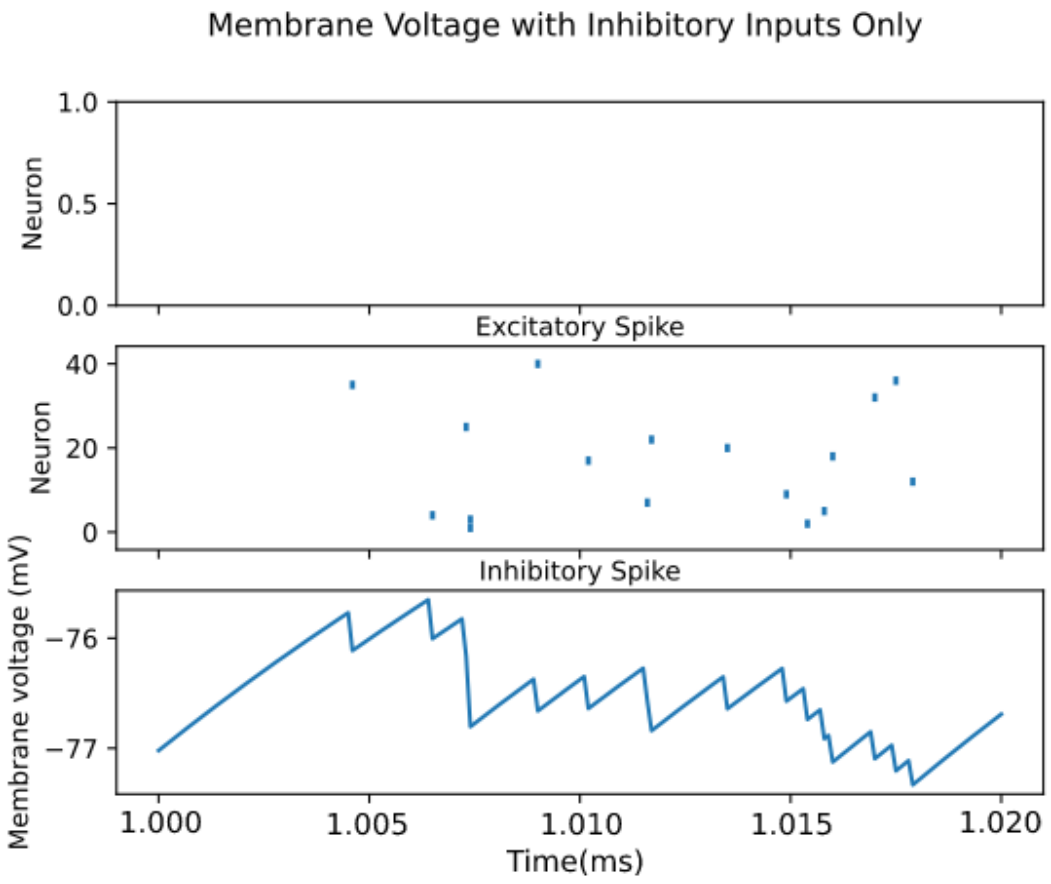

Figure 2: Membrane Voltage of Target Neuron Given Excitatory Input Neurons Only and Inhibitory Input Neurons Only. From top to bottom, the three sections of each panel show the raster of the spikes in excitatory neurons, the raster of the spikes in the inhibitory neurons, and the resulting post-synaptic potential in the model target neuron. I select data starting from 1 second, as it achieves a rather steady-state condition, which alleviates any worries about start-up conditions.

The graphs in Figure 2 serve as proof of concept of the target neuron's response to excitatory and inhibitory inputs. With excitatory input neurons only and no inhibitory inputs (Figure 2a), the target neuron fires a spike (marked by red vertical line) after consecutive stimulation from excitatory inputs in multiple neurons. The target neuron's membrane voltage returns to its resting potential after firing a spike and retains that membrane voltage until the afterhyperpolarization period ends. With inhibitory input neurons only and no excitatory inputs (Figure 2b), the target neuron hasn't reached reversal potential, as the inhibitory post-synaptic potential drags the membrane voltage back towards resting potential. Thus, continuous inhibition creates a fluctuating pattern of low membrane voltage and prevents spiking.

a. b. c.

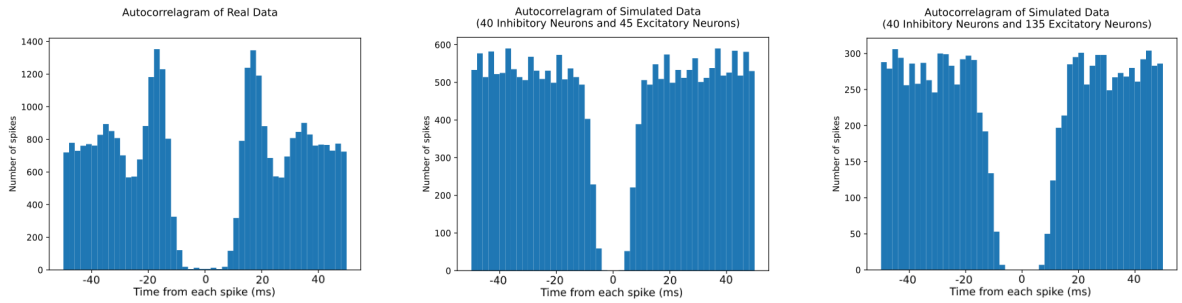

Figure 3: Autocorrelograms (ACG) of Real v.s. Simulated Data with 40 Inhibitory Neurons and Different Numbers of Excitatory Neurons. Figure 3a is the ACG of a real target neuron recording in a behaving animal. Figure 3b is the ACG of a model target neuron with 45 excitatory neurons and 40 inhibitory neurons, without any attempt to reproduce the response of the real neuron. Figure 3c is the ACG of a model target neuron with 135 excitatory neurons and 40 inhibitory neurons. An ACG plots the time of neighboring spikes relative to the time of each spike in the full response of the real or model neuron and summarizes the discharge statistics of a neuron.

The autocorrelograms illustrated in Figure 3 provide useful information for summarizing and analyzing the randomness or non-randomness of the spike trains of a real or model neuron. By comparing the autocorrelogram of real neuron recordings to that of my simulated neural network model, I find that the plot for real data has a tall narrow peak at around 18 ms and a shorter wider peak at around 36 ms, while the plot for the model with 45 excitatory neurons has no peaks. This comparison demonstrates that the real neuron firing pattern is much more regular compared to the model, as it has a strong tendency to have an interspike interval of approximately 18 ms, corresponding to a firing rate of around 55 spikes/s. The main challenge for the rest of my project is to discover how to make the model neuron's ACG more similar to that of the real target neuron.

To tackle this problem, the first approach I use is to increase the number of excitatory neurons to 135 neurons and adjust the excitatory synapse conductance to 1/3 of its original assigned value. The rationale is that more excitatory neurons reduce the collective variance of these neurons' spike pattern while preserving the randomness of the individual neuron's spike pattern. In addition, multiplying the number of excitatory neurons by 3 while dividing the excitatory synapse conductance by 3 preserves the equation for updating membrane voltage. However, there are still significant differences between the plot of real data versus that of the adjusted model with 135 excitatory neurons (Figure 3c). I conclude that the variance of the excitatory inputs is not a factor in generating regular firing in the target neurons, so other approaches will be needed.

a. b. c. d.

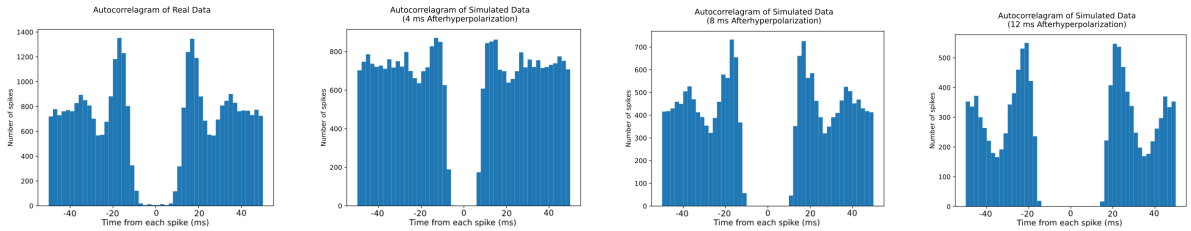

Figure 4. Autocorrelograms (ACG) of Real v.s. Simulated Data (135 Excitatory Neurons, 40 Inhibitory Neurons) with 4 ms, 8 ms, 12 ms Afterhyperpolarization Periods from Left to Right. To find the appropriate length of afterhyperpolarization period, I compare the ACG of a real target neuron (Figure 4a) to the ACG of a model target neuron with 4 ms, 8 ms, 12 ms afterhyperpolarization periods respectively (Figure 4b-d).

My next approach was to adjust the duration of the afterhyperpolarization period that held the membrane potential of the target neurons in a hyperpolarized state for a given period of time after each spike. With a 4 ms afterhyperpolarization period, the ACG of the model neuron only has one peak around 15 ms away from each spike. The spike train of the model neuron is much more random compared to the real neuron, as the frequency remains high for different times from each spike. With an 8 ms afterhyperpolarization period, the ACG of the model neuron has 2 peaks, one around 18 ms and another around 36 ms, very similar to the ACG of the real neuron. In addition, the shape and spread of the ACG of the real neuron and the ACG of the model neuron with an 8 ms afterhyperpolarization period are similar. With a 12 ms afterhyperpolarization period, the ACG of the model neuron has 2 peaks, but one peak around 20 ms and another peak around 45 ms. The peaks are also wider than that of the ACG of the real neuron. This shows that the model neuron with a 12 ms afterhyperpolarization period has lower spike rates and more randomness in the spike train compared to the real neuron. Thus, I find that the ACG of a model neuron with 8 ms afterhyperpolarization period is the closest to the ACG of the real neuron, and 8 ms is the most appropriate length of afterhyperpolarization period for simulating our real neuron.

a. b. c. d.

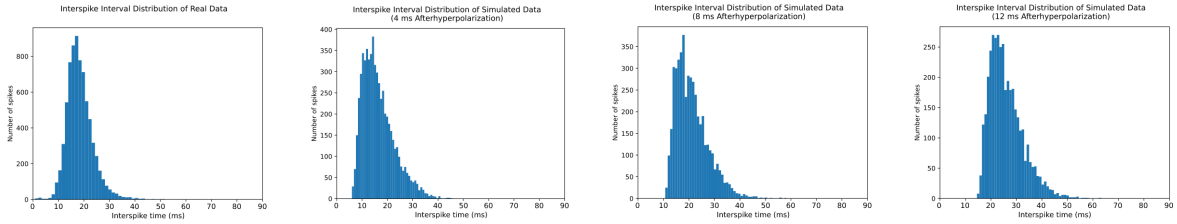

Figure 5. Interspike Interval Distributions (ISI) of Real v.s. Simulated Data (135 Excitatory Neurons, 40 Inhibitory Neurons) with 4 ms, 8 ms, 12 ms Afterhyperpolarization Periods from Left to Right. Figure 5a: Data from real floccular target neuron. Figure 5b-d: Simulations of model neurons with 4, 8, or 12 ms afterhyperpolarization periods.

To further confirm that 8 ms is the correct choice for the duration of the afterhyperpolarization, I generate interspike interval (ISI) plots to compare the real neuron with the model neurons. The ISI plots for the model neuron with different lengths of afterhyperpolarization period don't vary much. They have a similar range of around 10-50 ms of interspike time and a similar shape. However, with a 4 ms afterhyperpolarization period, the center of the ISI for the model neuron is around 13 ms. With a 12 ms afterhyperpolarization period, the center of the ISI for the model neuron is around 22 ms. With a 8 ms afterhyperpolarization period, the center of the ISI for the model neuron is around 18 ms, most similar to that of the real neuron, which shows that the average spike rate of a model neuron with a 8 ms afterhyperpolarization period is most similar to that of the real neuron. Thus, I find that the ISI of a model neuron with a 8 ms afterhyperpolarization period is the closest to the ISI of a real neuron, which confirms that 8 ms is the most appropriate length of afterhyperpolarization period for simulating our real neuron.

a. b.

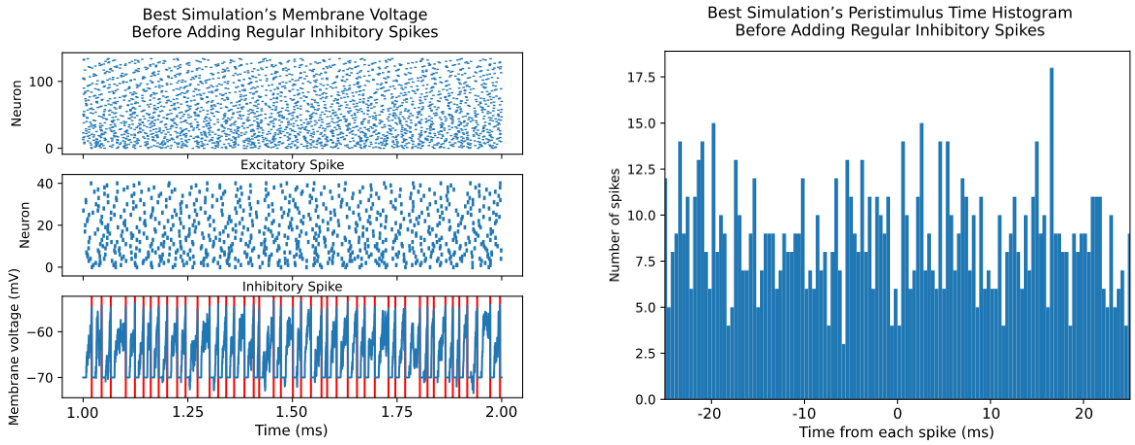

c.

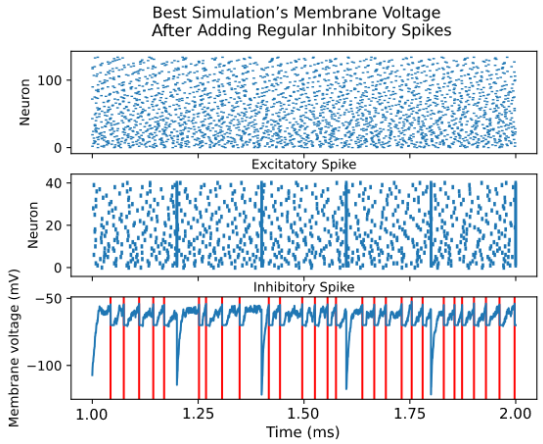

d.

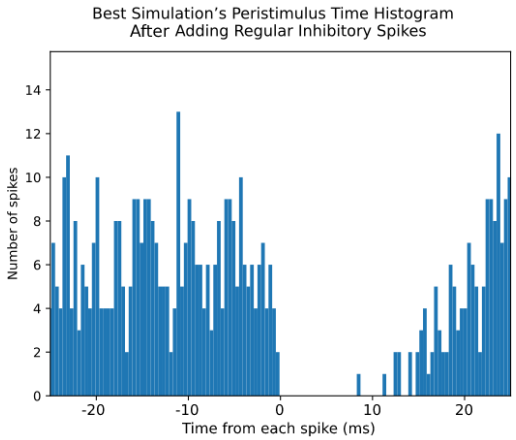

Figure 6. Best Simulation's Membrane Voltage and Peristimulus Time Histogram (PSTH) Before and After Adding Regular Inhibitory Spikes: Figure 6a-b: Membrane voltage and PSTH before adding regular inhibitory spikes. Figure 6c-d: Membrane voltage and PSTH after adding regular inhibitory spikes.

After I build a model target neuron that successfully reproduces the response of the real neuron, I start to investigate the relationship between the synchrony of inhibitory inputs and the response of the target neuron with my model. I add an inhibitory spike to all the inhibitory input neurons every 200 ms, the membrane voltage of the target neuron goes down rapidly at the time of the spike due to synchronous inhibition. I summarize the target neuron's response with PSTH plots. PSTH plots are useful for visualizing the rate and timing of neuronal spike discharges in relation to an external stimulus or event. Comparing the 2 PSTH plots, before and after synchronous inhibition, I find that the synchronous inhibition causes an around 8 ms period of zero spike right after the time of stimulation. This demonstrates that the synchronization of inhibitory inputs indeed has an effect on the response of the target neuron.

a.

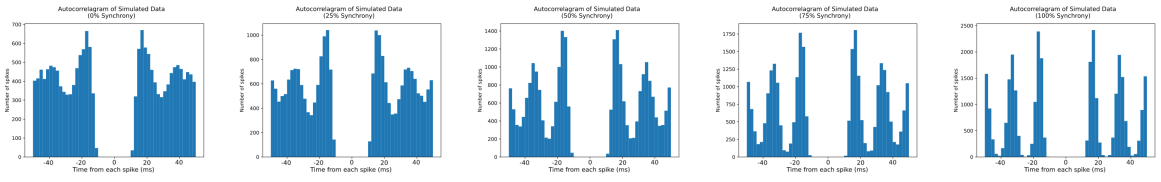

b.

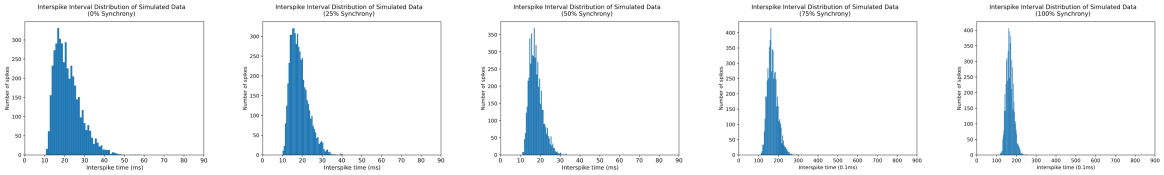

Figure 7. Best simulation's Autocorrelograms (ACG) and Interspike Interval Distributions (ISI) with Different Levels of Synchrony (0%, 25%, 50%, 75%, 100% from Left to Right): Figure 7a: ACGs for the model with different levels of synchrony. Figure 7b: ISIs for the model with different levels of synchrony. I create the level of synchrony by setting a percentage of inhibitory input neurons to have the exact same spike pattern, while others have randomized spike patterns as defined in the beginning.

In Figure 7a, with increasing levels of synchrony from left to right, the number of peaks in the ACGs increases from 2 to 3, the width of peaks gets narrower, and the values of the peaks increase. The time from each spike gets more concentrated on values around 17 ms, 34 ms, 51 ms, which shows a consistent pattern of the target neuron's spike pattern exhibiting less randomness given increasing levels of synchrony from the inputs. When we look at Figure 7b, with increasing levels of synchrony from left to right, the center of the ISI plots remain to be at around 17 ms, meaning the level of synchrony of the inputs doesn't affect the mean firing rate of the target neuron. However, the spread of the distributions keeps getting smaller. This shows that with more synchronization in the inhibitory inputs, the target neuron's spike rate becomes more stable and has less variability. The closest resemblance to the data from the real neuron occurs with zero synchrony. I conclude that synchronous inhibitory inputs are not required to account for the firing of real target neurons recorded in vivo.

DISCUSSION

In this paper, I model a real target neuron recording in a behaving animal without using synchrony in my model. I do so by finding appropriate values for synapse conductance and reversal potential, adjusting the number of excitatory neurons in the network, and finding the best value for the length of the afterhyperpolarization period. I acknowledge that there are many different ways to model the neuron, and my model is just a simple way among them. By comparing autocorrelograms, interspike interval distributions, and peristimulus time histograms that summarize the resting discharge properties of the real target neuron and the model target neuron, I show that my model is a valid model to use.

Using my model, I show that little or no inhibitory input synchrony is required to simulate the resting firing statistics of the real neuron, and that the synchrony of inhibitory inputs may not be a major component of the neural code for the output from the cerebellum. Further, I show that resting firing statistics provide a sensitive assay of the effects of synchrony in a neuron's inhibitory inputs. Yet, other tests that are not available to me might involve the responses of the inhibitory neurons and the target neuron during a relevant behavior. Indeed, the most sensitive probe would be an in vivo experiment with synchronous stimulation of Purkinje cells and recording from the target neuron. Or, alternatively, one might record simultaneously from

multiple nearby Purkinje cells and assay the degree of synchrony [6]. Such experiments might be the next steps to verify my findings.

Finally, I recognize that the cerebellum is only one brain structure and that the rules I have discovered may or may not generalize to signaling in the brain more widely (e.g. [7], [8]). I hope the results in the cerebellum can generalize to the entire brain, but this is up to other neurologists and researchers to verify.

BIBLIOGRAPHY

[1] Ito, Masao. *Cerebellar control of the vestibulo-ocular reflex--around the flocculus hypothesis*. *Annual Review of Neuroscience* Vol. 5:275-297 (1982). DOI: 10.1146/annurev.ne.05.030182.001423. PMID: 6803651.

[2] Kahlon, Maninder and Lisberger, Stephen G. *Changes in the responses of Purkinje cells in the floccular complex of monkeys after motor learning in smooth pursuit eye movements*. *Journal of Neurophysiology* 84(6):2945-60 (December 2000). DOI: 10.1152/jn.2000.84.6.2945. PMID: 11110823; PMCID: PMC2581904.

[3] Heck, Detlef H. et al. *The Neuronal Code(s) of the Cerebellum*. *Journal of Neuroscience* 33 (45) 17603-17609 (November 2013). DOI: 10.1523/JNEUROSCI.2759-13.2013

[4] Person, Abigail and Raman, Indira. *Purkinje neuron synchrony elicits time-locked spiking in the cerebellar nuclei*. *Nature* 481, 502–505 (2012). DOI: 10.1038/nature10732.

[5] Steuber, Volker and Jaeger, Dieter. *Modeling the generation of output by the cerebellar nuclei*. *Neural Networks* Volume 47, 112-119 (2013). DOI: 10.1016/j.neunet.2012.11.006.

[6] Herzfeld, David J. et al. *Rate versus synchrony codes for cerebellar control of motor behavior*. *bioRxiv [Preprint]* 2023.02.17.529019 (February 2023). DOI: 10.1101/2023.02.17.529019. PMID: 36824885; PMCID: PMC9949136.

[7] Long, Michael A. et al. *Support for a synaptic chain model of neuronal sequence generation*. *Nature* 468, 394–399 (2010). DOI: 10.1038/nature09514.

[8] Sober, Samuel J. et al. *Millisecond Spike Timing Codes for Motor Control*. Trends in Neurosciences. 41(10):644-648 (October 2018). DOI: 10.1016/j.tins.2018.08.010. PMID: 30274598; PMCID: PMC6352894.